7

8

9

10 **Increasing the reaction kinetics of alkali activated fly ash binders for**

11 **stabilisation of a silty sand pavement sub-base**

12

13 [a,*] Sara Rios; [b] Nuno Cristelo; [c] Tiago Miranda; [d] Nuno Araújo; [e] Joel Oliveira;

14 [d] Ernesto Lucas

15

16 [a] *Post-Doc Research fellow, CONSTRUCT-GEO, Department of Civil Engineering, Faculty of*
17 *Engineering, University of Porto, 4200-465 Porto, Portugal*
18 [*] Corresponding author
19 E-mail address: sara.rios@fe.up.pt
20
21 [b] *Assistant Professor, CQVR, Department of Engineering, University of Trás-os-Montes e*
22 *Alto Douro, 5001-801 Vila Real, Portugal*
23
24 [c] *Assistant Professor, ISISE, Department of Civil Engineering, University of Minho,*
25 *4800-058 Guimarães, Portugal*
26
27 [d] *Assistant Professor, ISISE, Department of Civil Engineering, University of Minho,*
28 *4800-058 Guimarães, Portugal*
29
30 [e] *Assistant Professor, CTAC, Department of Civil Engineering, University of Minho,*
31 *4800-058 Guimarães, Portugal*
32
33 [d] PhD student, *CQVR, Department of Engineering, University of Trás-os-Montes e Alto*
34 *Douro, 5001-801 Vila Real, Portugal*
35

36 **Abstract**

37

38 The paper addresses several options to improve the reaction kinetics of alkali activated low

39 calcium fly ash binders for soil stabilisation in road platforms. For that purpose, an experimental

40 program was established to assess the strength evolution, with time, of different binders, based

41 on ash, lime, sodium chloride and alkali solutions, applied in the stabilisation of a silty sand.

42 The tests included unconfined compression strength tests, triaxial tests and seismic wave

43 measurements performed at different curing periods. The results were compared with a binder

44 made of Portland cement and a commercial additive specifically designed for soil stabilization

45 in road applications. The activated ash mixtures with lime were the most performing producing

46 a significant increase in the reactions development and, consequently, in the strength gain rate.

47 The sodium chloride significantly improved the lime and lime-ash mixtures, but provided only

48 a slight improvement in the activated ash mixtures.

49

50

51 Keywords: soil stabilization; fly ash; lime; alkaline activation, Portland cement

52

53

Introduction

With the worldwide increase in constructed surface area, the need for local soil stabilization or improvement keeps growing. Different methods have been used for decades, and several of those are still being improved and refined, while new ones keep arising as technology progresses. According to Mitchell (1981) and van Impe (1989) the stabilisation / improvement techniques can be divided in the following groups: consolidation; grouting; mechanical, chemical and physical stabilisation; and soil reinforcement. Almost all of the mentioned groups comprise one or more techniques that can be very efficiently applied in transport infrastructures. Compaction, consolidation, grouting and soil reinforcement can be used to improve the bearing capacity and deformability properties of embankments or slopes; while mechanical (surface compaction) and chemical stabilisation are very common when dealing with superficial layers.

In particular, chemical stabilisation is very efficient when the soils available nearby cannot present an adequate performance based only on mechanical stabilisation. The use of a soil-binder combination specifically developed for subgrade layers can significantly increase its strength and stiffness, avoiding the extraction of more performing materials from distant locations (Ingles & Metcalf, 1972; Little, 1995; Sherwood, 1993; Little & Nair, 2009).

The most common binders for surface stabilisation are based on Ordinary Portland cement (OPC) and/or lime (Petry & Little, 2002; Xing et al, 2009). Due to the pozzolanic properties of common clay minerals, the high amount of calcium present in both slaked and unslaked lime makes it a very effective option to decrease plasticity and increase workability, with also some significant strength and stiffness increase if dry weight percentages above 6% are used (Cristelo et al, 2009; Little et al, 2010; Al-Mukhtar et al, 2014; Gullu, 2015; Han & Cheng, 2015; Elkady, 2016). When dealing with silty to sandy soils, OPC is usually the most interesting option (Consoli et al, 2011a; Bahar et al, 2004; Goodary et al, 2012; Rios et al., 2012, 2014). However, if a significant increase in strength is necessary in a clayey soil, the

80   most consensual strategy is probably to mix the soil with lime, before mixing the resulting

81   granular material with OPC (Horpibulsuk et al., 2006; Yusuf et al, 2001; Yong & Ouhadi,

82   2007; Oza & Gundaliya, 2013; Khemissa and Mahamedi, 2014; Saride et al, 2013). Several

83   binders have been tested, with more or less success (Kolias et al, 2005; Basha et al 2005;

84   Kaniraj & Havanagi, 1999; Kamei et al, 2013; Yilmaz & Ozaydin, 2013; Gurbuz et al, 2015),

85   but in almost every case OPC plays a major role in the stabilisation process.

86   Based on the literature review, it becomes clear that cement is the most important

87   constituent in chemical stabilisation of soil subbases, producing significant strength and

88   stiffness increase with little or no setbacks whatsoever. Nevertheless, the decreasing tolerance

89   regarding the environmental concern has the production of clinker as a major target, mostly

90   due to the high amount of CO_2 released. A value between 5% and 8% of the overall CO_2

91   released to the atmosphere is estimated to be originated by OPC production (Provis & van

92   Deventer, 2014; Scrivener & Kirkpatrick, 2008). Therefore, there is an ongoing research

93   effort targeting the development of more sustainable binders (Juenger et al., 2011). In

94   particular, the use of waste materials is highly encouraged, since it allows an increase in

95   resource efficiency, while contributing also to enhancing the circular economy (by reducing

96   landfilled waste).

97   The alkaline activation technique is particularly adequate to create binders based on

98   residues, such as fly ash or ground granulated blast furnace slag, which constitute very

99   effective options due to their amorphous aluminosilicate microstructure. It consists on a

100   reaction between aluminosilicate materials and alkali or alkali-based earth substances, such as

101   sodium (Na) or potassium (K), or an alkaline earth ion, such as calcium (Ca). The reactions

102   can be summarized in the following sequence. First, there is the destruction, by the high

103   hydroxyl (OH-) concentration in the alkaline medium, of the Si-O-Si, Al-O-Al and Al-O-Si

104   covalent bonds present in the vitreous phase of the original semi-amorphous aluminosilicate

105   (i.e. the precursor). The Si and Al ions are released into the solution as they become available

4

106 and; at the same time, the alkaline cations – usually Na+ or K+, depending on the activator –

107 compensate the excess negative charges associated with the modification of the aluminium

108 coordination during the dissolution phase. The resulting products accumulate for a period of

109 time, forming an ion-rich solution, which finally precipitates and reorganizes into more stable

110 and ordered Si-O-Al and Si-O-Si structures. If calcium is predominant, relatively to the

111 sodium or potassium, the dissolved Al-Si ions will diffuse from any solid surface, which

112 favours the production of a C-S-H gel phase. Otherwise, the Si and Al ions will be able to

113 accumulate around the nuclei points, sharing all the oxygen ions and forming a Si-O-Al and

114 Si-O-Si three-dimensional structure (the formation of Al-O-Al is not favoured). The resulting

115 product is an amorphous alumina-silicate gel, which evolves, with curing time and

116 crystallization, from an Al-rich phase to a Si-rich phase. The crystallization, starting almost

117 immediately after the precipitation, is responsible for the hardening of the gel, which

118 eventually matures into alkaline cement, with pre-zeolite as secondary products (Fernández-

119 Jiménez and Palomo, 2005; Fernández-Jiménez et al., 2006). The precursor should always be

120 submitted to a previous thermal treatment, capable of inducing the loss of constituent water

121 and the subsequent re-coordination of the aluminium and oxygen ions, transforming an

122 originally crystalline structure into an amorphous one, more susceptible to further chemical

123 reactions. The relative presence of calcium in the precursor and/or in the activator is very

124 important, since the speed of the reactions is highly dependent on the type of aluminosilicate

125 gel being formed, either N-A-S-H or C-S-H. The former needs longer periods in order to

126 mature into a stable and reliable matrix, while the latter has curing / developing periods

127 similar to those obtained with cement-based binders (Dombrowski et al, 2007; Garcia-Lodeiro

128 et al., 2013).

129   Alkaline activation has recently started to be applied in soil stabilisation applications,

130 using fly ash as the precursor, allowing significant strength gains (Zhang et al, 2013; Sukmak

131 et al., 2013, 2015; Cristelo et al., 2011, 2012a, 2013; Silva et al., 2013; Rao and Acharya,

132 2014; Yi et al., 2015; Rios et al., 2015; Phummiphan et al., 2016), but also financial and

133 environmental benefits, which proved very competitive when compared with lime or cement-

134 based soil stabilizers (Cristelo et al., 2015). Other works were also recently published using

135 alkaline activation to stabilise other types of granular materials that do not include soils such

136 as construction and demolition waste (Mohammadinia et al., 2015; Arulrajah et al., 2016),

137 coffee grounds (Kua et al., 2016), or recycled asphalt pavement (Saride et al., 2016, Hoy et

138 al., 2016). However, constrains related with short deadlines regarding the entry into operation

139 of most infrastructures, and namely road and railways, often require tight construction

140 periods, which hinders the use of alkali activated low calcium (class F) fly ash, based on the

141 mentioned slower reaction kinetics of the N-A-S-H gel, when compared with the C-S-H gel.

142 However, in the presence of enough calcium, the two systems are very compatible, and

143 several studies have focused on the characterisation of their interaction and coexistence

144 (Garcia-Lodeiro et al., 2009, 2011; Puligilla & Mondal, 2013; Bui et al, 2015).

145   The need to improve the reaction kinetics of alkali activated class F fly ash binders

146 constituted the motivation of the present paper. A viable method would have been the use of

147 activated class C (high calcium) fly ash, which has proved very efficient for the stabilisation

148 of a lateritic soil for bound pavement application (Phummiphan et al., 2016). However,

149 assuming that such high calcium fly ash is not available, the need to develop alternative

150 procedures to increase the strength gain rate is obvious. Therefore, several mixtures were

151 prepared to find an effective method to increase the strength gain rate of a silty-sand stabilised

152 with low calcium, alkali activated fly ash.

153   Some authors (Ghosh and Subarao, 2001; Kumar et al., 2007; Samaras et al., 2008;

154 Consoli et al., 2011b) have reported that a significant strength increase of lime stabilised

155 clayey soils can be achieved with the addition of fly ash, enhancing the pozzolanic reaction,

156 which is the main responsible for the mechanical properties of the soil-lime mixture.

157 Additionally, several authors (Ramesh et al., 1999; Narendra et al., 2003; Cristelo et al., 2009)

158 have concluded that the formation of such pozzolanic reaction compounds is faster in the

159 presence of sodium chloride. According to these authors, this can be attributed to the

160 increased solubility of the silica and to the formation of sodium calcium silicate hydrate (N-S-

161 C-H), more voluminous and with a higher water-holding capacity than the well-known C-S-H

162 gel, formed in the sole presence of soil and lime. Based on these findings regarding the role of

163 fly ash and sodium chloride on soil stabilisation, additional mixtures were considered, for

164 comparison purposes, in which fly ash was added to soil-lime mixtures, with and without the

165 addition of sodium chloride. The addition of sodium chloride was also used to prepare

166 activated fly ash mixtures. Finally, a specific commercial additive for road pavement

167 applications (recently available in the market called RoadCem®) was mixed with Portland

168 cement, and the resulting binder was used to prepare some additional specimens. The result

169 was regarded as a threshold value to which the mixtures developed in the present work were

170 compared with.

171   In short, the following mixtures were conceptually analysed throughout the paper:

172   • Lime alone and with sodium chloride;

173   • No-activated fly ash and lime with and without sodium chloride;

174   • Activated ash and lime with and without sodium chloride;

175   • RoadCem® and Portland cement

176

177 **Experimental program**

178 *Soil identification*

179 The work presented in this paper was based on a soil from Poland, which was fully

180 characterized at the beginning of the experimental program described below. Typical

181 geotechnical identification tests were performed in order to determine the particle size

182 distribution, Atterberg's limits, Modified Proctor compaction parameters, and the California

183 Bearing Ratio (CBR). The particle size distribution curve (Figure 1) evidences a well graded

184 soil, with almost 50% fines – silt (27.8%) and clay (16%), which was classified as a SC-SM -

185 silty sand according to ASTM (2011) D 2487-11. Other parameters are summarised in **Erro!**

186 **A origem da referência não foi encontrada.**.

187   The minerology was examined by a PANalytical X'Pert Pro diffractometer, fitted with

188 an X'Celerator detector and secondary monochromator. The scans covered a 2 Θ range of 10º

189 to 80º, with a nominal step size of 0.017º and 100 s/step. CuK α radiation, with a wavelength

190 of $\lambda = 1.5418$ Å, was used. Qualitative phase identification was made using High Score Plus

191 software, which utilises the International Centre for Diffraction Data Power Diffraction File

192 database (ICDD PDF-2, Sets 1-49, 1999) as a reference. X-Ray diffraction patterns of the soil

193 showed the presence of quartz and muscovite on the mineralogical composition.

194 *Characterisation of the binders*

195 The fly ash was provided by a Portuguese thermo-electric power plant and, based on ASTM C

196 618 (2015), was classified as Class F due to the low calcium content as it is expressed on Table

197 2. Hydrated lime provided by the company Lusical, Lhoist was also used. The particle size

198 distribution of both lime and fly ash are plotted in Figure 1 together with the soil particle

199 analysis. The activator solution used was composed by sodium hydroxide and sodium silicate

200 . The former was supplied in pellets, with a specific gravity of 2.13 at 20ºC (99 wt. %), as

201 indicated by the supplier, which was then dissolved in water to pre-determined concentration

202 of 12.5 molal. The sodium silicate technical sheet indicates a unit weight of 1.464 g/cm^3 at

203 20ºC, a SiO_2/Na_2O weight ratio of 2.0 (molar oxide ratio of 2.063) and a Na_2O concentration

204 in the solution of 13.0%. A sodium silicate to sodium hydroxide ratio of 0.5 was always

205 considered. Deionised water was used in every mixture prepared during the work presented.

206   Some mixtures were also prepared with Ordinary Portland cement, type CEM I-42.5R,

207   together with a commercial soil stabiliser, specifically designed for road pavements, named

208   RoadCem®. This product can be described as a fine grain additive, based on alkali earth

209   metals and synthetic zeolites, complemented with a complex activator. Based on the technical

210   sheet, this product modifies and extends the chemistry of the cement hydration process and

211   extends the crystallization process by forming long needle crystalline structures. It is able to

212   delay or to speed up the hydration process of cement and can thus be used as a tool to custom

213   design the mixes of required performance. It is always used in combination with cement

214   and/or other pozzolanic materials (Marjanovic et al., 2009).

215   *Specimen preparation and mixture composition*

216   Preparation of the soil included drying and de-flocculation by hand. The solids were then dry

217   mixed for 10 min in a Hobart counter mixer, and the liquid phase was carefully added,

218   requiring an additional 10 min mixing period. Cylindrical specimens with 70 mm in diameter

219   and 140 mm in height were then compacted for uniaxial and triaxial compression strength

220   tests, using static compaction according to EN 13286-53 CEN (2004a). The top and bottom of

221   the moulds were then covered with cling film and the specimens were left for forty-eight

222   hours before the mould could be removed. After demoulding the specimens were allowed to

223   cure for longer in the same conditions: at 20ºC ± 1ºC and 90% RH ± 3%.

224   Identification of the mixtures is presented in **Erro! A origem da referência não foi**

225   **encontrada.**. Each component of the solid phase is defined as a percentage of the total mass

226   of solids, and the water content as the ratio between the amount of water and the amount of

227   solids. All mixtures were identified using the following code: 'S' (soil); 'FA' (fly ash); 'L'

228   (lime); 'C' (sodium chloride); 'AA' (alkali activated); 'OPC' (Ordinary Portland cement) and

229   'RC' (RoadCem). Some of these letters were followed by a number, indicating the respective

230   dosage. In the first step the specimens were moulded on the maximum dry unit weight and

231   optimum water content, obtained for the soil, using a modified Proctor test (**Erro! A origem**

232   **da referência não foi encontrada.**), but in the second and third steps the presence of lime

233   and the consequent cationic exchange and flocculation prevented a higher compaction degree.

234   Therefore, in steps 2 and 3, mixtures were moulded at 88% of the optimum dry unit weight,

235   corresponding to a maximum dry unit weight of 18.8 kN/m^3. All specimens were moulded

236   with a water content of 5%, corresponding to 88% value in the Proctor curve, with the

237   exception of the geopolymeric mixtures, which required a higher water content in order to

238   fulfil the criteria related with the activator/ash ratios. For comparison purposes, a specimen of

239   unstabilised soil was also prepared, being compacted at 88% of the Proctor maximum value.

240   *Uniaxial compression strength testing*

241   An Instron® electro-mechanical load frame , fitted with a 25 kN load cell, was used for the

242   unconfined compressive strength tests. The tests were carried out according to EN 13286-41

243   (CEN, 2003a) under monotonic displacement control, at a rate of 2 mm/s, and the entire

244   stress-strain curve was obtained from each test.

245   *Triaxial testing*

246   Consolidated undrained triaxial compression tests (CU), following CEN ISO/TS 17892-9

247   (CEN, 2004b), were performed on the original soil, after isotropic effective consolidation

248   stresses (σ'_c) of 33 kPa, 100 kPa and 300 kPa. Additionally, drained triaxial compression tests

249   (CD) were performed in two of the bounded mixtures – S_FA15_L5_AA3 and

250   S_FA10_L5_AA3 – previously cured for 28 days, using effective isotropic consolidation

251   stresses of 50 kPa, 100 kPa and 200 kPa. These particular mixtures were chosen due to the

252   fact that they reached the most performing behaviour in the UCS tests.

253   After the installation in the triaxial cell, water was allowed to percolate through the

254   specimen until a volume of water higher than twice the volume of voids was obtained. This

255 facilitated saturation because removed the air bubbles present in the specimen and in the

256 tubing system. Then, the saturation followed where cell and back pressures were increased

257 simultaneously at a rate of 30 kPa per hour keeping an effective stress of 10 kPa, until cell

258 and back pressure achieved 410 and 400 kPa respectively. This back-pressure value was kept

259 constant during 24 h, assuring full-saturation which was verified by the B Skempton

260 parameter which was close to 1.

261   The same servo-hydraulic load frame used for UCS tests, fitted with a 25 kN load cell,

262 was used to apply the deviatoric load, under monotonic displacement control, at a rate of

263 0.01 mm/min. The axial deformation was measured by two Linear Displacement

264 Transformers (LDTs) (Goto et al., 1991), while an additional LDT was installed to monitor

265 the radial deformation as illustrated in Figure 2.

266 *Seismic waves*

267 Compression seismic (P) wave velocities were measured by ultrasonic non-destructive

268 transducers, after curing periods of 12, 24 and 48 h, and then after 3, 7, 14 and 28 days in

269 some of the specimens tested in unconfined compression as expressed in **Erro! A origem da**

270 **referência não foi encontrada.**. A commercially available equipment was used, consisting of

271 axially aligned piezoelectric transducers, with a nominal frequency of 54 kHz and 30 mm in

272 diameter; a waveform generator; an amplifier and an interval timer with a direct reading

273 digital display, which showed the P-wave velocity (V_P) in real time. An oscilloscope would

274 have been preferable, due to the lower definition of the pulse wave when travelling through

275 heterogeneous materials, like soil. However, such equipment was not available. The

276 equipment has an excitation voltage of 1000V and a resolution of 0.1μs. The equipment

277 identified automatically the P wave travel time without any operator interference, and

278 therefore no specific analysis was needed as in other advanced devices (Camacho-Tauta et al.,

279 2015). In this case, standard EN 12504-4 (CEN, 2003b) was used as general reference, and

280 calibration of the transducers was automatically performed by the equipment, using a metallic

281 rod with a known P-wave travelling time of 20.9μs. The measurements were taken along the

282 longitudinal axis of the specimens, with the specimen vertically aligned and the transducers

283 installed on opposite faces. The acoustic coupling between the transducers and the specimen

284 was obtained using ultrasound gel, while firmly pressing the transducers against the top

285 surfaces of the specimen. Each result presented is the average of ten consecutive readings.

286

287 **Experimental results**

288 *Unconfined compressive strength*

289 In the first step of **Erro! A origem da referência não foi encontrada.**, designed to

290 obtain a guideline in terms of time needed for the reaction to produce meaningful UCS

291 results, three different liquid/solids ratios were considered, by varying the liquid phase (the

292 solids were kept at 85% S + 15% FA). Based on the results obtained, further activated

293 mixtures were performed with an activator / ash ratio equal to 0.707 (the criteria for such

294 value are discussed later in the text).

295 In the second step, the soil was mixed with different binders in order to evaluate the

296 effect, on the reaction's kinetics, of each of the combinations proposed. Mixtures of soil-lime

297 as well as soil-lime-fly ash (both with and without sodium chloride) were first performed with

298 deionised water as the only constituent of the liquid phase. Then, the fly ash and fly ash-lime

299 mixtures were prepared with the activator as the only constituent of the liquid phase.

300 A third and final step was then designed to reduce the mixture cost which included the

301 reduction of the fly ash to 10% of the total solids (and consequently, a lower quantity of

302 activator solution), while using only one lime percentage (10%) and 1% of sodium chloride.

303 Also included in this final step were the OPC + RC mixtures.

304   At least 3 specimens of each condition were always moulded and tested so that the

305   presented data corresponds to the average of three tests, improving the statistical confidence

306   on the results. A unique curing period of 28 days was considered during the first step, while

307   three different curing periods of 3, 7 and 28 days were considered in the second step. In the

308   third step, L + FA specimens were tested after 7 days, while OPC + RC specimens were cured

309   for 3, 7 and 28 days as expressed in **Erro! A origem da referência não foi encontrada.**

310   The results obtained in step 1 with distinct activator contents and a ash content of 15% was

311   aimed to evaluate the effect of the Na_2O/ash ratio on UCS (Cristelo et al., 2012a). As such,

312   activator/ash ratios of 0.943, 0.825 and 0.707 were considered, resulting in activator contents

313   (liquid/solids ratio) of 14.1%, 12.4%, and 10.6%. Since the three mixtures presented a

314   significant strength increase (Figure 3), the lowest activator content of 10.6% was selected for

315   the following steps, even though the activator content of 12.4% achieved higher strength. This

316   was due to the fact that a reduction in activator implies a reduction of the total cost of the

317   mixture, since the activator is, by a significant margin, the most expensive component.

318   Figure 4 illustrates the strength results obtained in step 2, as well as the corresponding secant

319   stiffness modulus at 50% of the maximum strength (E_{50}). This parameter is essential to

320   characterise the material's constitutive model included in any finite element code, and

321   therefore its calculation is extremely useful for design purposes. With a few exceptions, the

322   mixtures with lower and higher strength values presented also lower and higher stiffness

323   values, respectively. Mohammadinia et al. (2014) have reported a E_{50}/UCS ratio around 1000

324   for cement-treated construction and demolition materials but in this case the ratio is closer to

325   100 probably due to a finer grading of the soil.

326   Note the significantly higher strength, after every curing period, achieved by the

327   mixtures with both lime and activated ash. While the mixture with activated ash achieved

328   similar strength values to those obtained by the lime and lime-fly ash mixtures, the addition of

329   lime to the former resulted in a 4 times strength increase. This is a consequence of the faster

330   reactions in C-S-H systems, relatively to N-A-S-H systems, as observed by the authors

331   Cristelo et al. (2012b) during a previous work that compared the strength gain rate motivated

332   by the activation of class C and class F fly ash.

333   Considering the existing design guidelines for roads, both the Portuguese road

334   specifications (JAE, 1995) and the French (GTS, 2000) classification chart for soil-cement

335   mixtures, suggest a minimum indirect tensile strength of 0.2 or 0.3 MPa, depending whether

336   in situ or plant mixing is used. These values can be converted into UCS values of 2 and

337   3 MPa assuming a ITS/UCS=10%. The GTS (2000) specification also adds the need to have

338   1 MPa at 7 days of curing. Using these values as target for design, as expressed in Figure 4, it

339   becomes clear that the soil-lime mixture do not fulfil these aims, while the soil-lime-ash

340   mixtures stay slightly above these limits. For higher performances, corresponding to higher

341   class treated layers as expressed in GTS (2000), activated ash mixtures are needed.

342   A final third step was conducted to address the possible reduction of the economic and

343   financial cost of the binders, considering that most UCS values obtained were very

344   satisfactory and could be slightly reduced without compromising its mechanical performance.

345   This cost decrease was obtained with a reduction of the fly ash percentage to 10%, down from

346   the step 2 overall value of 15%. Note that a reduction in fly ash content does not represent a

347   significant economic or environmental saving, but the reduction of the alkaline solution

348   content needed to activate the fly ash is, indeed, significant in terms of both of these aspects.

349   Results presented in Figure 5 (after curing for 7 days) show that the mixtures with both lime

350   and activated ash remain as the most performing combinations, even relatively to those

351   mixtures based on both cement and RoadCem®.

352   ***Triaxial compression strength***

353   Figures 6 and 7 show the stress-strain curves obtained from the triaxial tests performed on the

soil and selected bounded mixtures (with lime and activated ash), respectively as indicated in **Erro! A origem da referência não foi encontrada.**. These soil-binder mixtures were selected based on the efficiency/cost ratio obtained from the results from the uniaxial compression tests presented above.

The soil presented a quasi-linear behaviour up to 29%, 27% or 14% of the maximum deviatoric stress, depending on the effective confining pressure applied of 33, 100 or 300 kPa, respectively. After this linear segment, the soil stiffness significantly decreases, due to yielding, reaching a zero value when the soil achieved a constant stress plateau at the 20% to 30% strain mark. **Erro! A origem da referência não foi encontrada.** presents the results of the stiffness modulus at 50% of the maximum deviatoric stress (E_{50}), a usual design parameter as explained before.

The bounded mixtures showed completely different stress-strain curves, which in this case are typical of cemented materials (Rios et al., 2014, 2015), with a peak stress at very low strain levels (between 0.15 and 0.30%), followed by a very abrupt strain softening due to bond degradation. The material stiffness does not seem to be very much affected by the effective confining pressure, indicating that, for this pressure range, the consolidation stress did not produce an increase in stiffness, but it did not damaged the cemented structure either. This behaviour, typical of cemented soils (e.g., Fernandez and Santamarina, 2001), is expressed in **Erro! A origem da referência não foi encontrada.** showing that the E_{50} stiffness modulus was very similar for the three tests on S_FA10_L5_AA3 specimens (approximately 3000 MPa) and also for the three tests on S_FA15_L5_AA3 specimens (approximately 4000 MPa). Note that the latter E_{50} value is almost 10 times higher than the values obtained with the unstabilized soil. Also very clear is the fact that the reduction in ash content (from 15% to 10%), had a strong influence on peak stress, which decreased between 30% to 40%, depending on the confining pressure.

379 *P-wave measurements*

380 The results obtained from the seismic wave measurements are presented in Figure 8 relating

381 the P wave velocity (V_P) with curing time. It should be noted that the specimens are not

382 saturated, and so the presented results do not represent the propagation velocity through the

383 water, but through the soil grains. Consequently, the positive evolution of V_P with curing time

384 is expected since V_P are directly related with the constrained modulus being therefore an

385 indirect measurement of stiffness. The relative position between the V_P values obtained in

386 each specimen is in agreement with the previous data presented in Figure 4, confirming the

387 sensibility of this measurement.

388 However, the major advantage of this data is that being a non-destructive method it is possible

389 to have several measurements through the curing period without needing further specimens.

390 Figure 8 shows that there is a significant improvement in the first 7 days of curing and then the

391 evolution continues at a smaller rate. This is especially relevant for alkali-activated ash mixtures

392 and for specimens with lime and sodium chloride.

393

394 **Discussion**

395 *Strength envelope of bounded and unbounded mixtures*

396 The strength increase resulting from the mixture with lime and activated ash can be quantified

397 in terms of the Mohr Coulomb failure criterion, namely from the resulting strength parameters

398 ϕ' (friction angle) and c' (cohesion). The peak and ultimate strength envelopes of the soil and

399 the selected bounded mixtures are presented in Figure 9, while the corresponding Mohr-

400 Coulomb parameters are summarized in **Erro! A origem da referência não foi encontrada.**.

401 It is possible to observe that the peak friction angle almost doubled, while the peak cohesion

402 intercept suffered also a significant increase, which is typical of cemented materials. At

16

403　ultimate states the strength of the bounded mixtures approaches that of the soil since the

404　cohesion intercept reduces drastically. However, the values of the ultimate state friction angle

405　are still significantly higher than those obtained for the unstabilized soil (peak or ultimate

406　state). This indicates that not all the artificially created bonds could be destroyed in the test,

407　instead forming small clusters that reduced the void volume between the soil particles.

408　*Effect of sodium chloride addition*

409　Figure 10 presents the Step 2 UCS related to the sodium chloride addition. The sodium

410　chloride was particularly effective in increasing the strength development rate of the non-

411　activated ash mixtures (S_L5 and S_FA15_L5), particularly after 28 days. The contribution of

412　the sodium chloride to the reaction kinetics is clear and, after 28 days, the addition of 1%

413　represents an UCS increase of 69% of the lime-based mixture and 59% of the lime and no-

414　activated ash mixture. Regarding the activated ash mixtures (S_FA15_L5_AA3), it appears

415　that the sodium chloride did not make a noticeable impact on strength increase, and has even

416　hindered the short-term (3 days) behaviour.

417　*Effect of lime percentage*

418　Step 2 tests also allowed to observe the effect of hydrated lime on the reaction kinetics of the

419　mixtures. Figure 11 compares the strength values obtained for the two lime percentages

420　considered (5% and 10%), for each of the three curing periods. The results indicate that the

421　increase in lime content affects the rate of strength development, especially between the 7th

422　and the 28th day. An increase of 5% in lime content, after 28 days curing, represented

423　strength increases of 40% (soil + lime + water), 56% (soil + ash + lime + water) and 22%

424　(soil + ash + lime + activator).

425 *Effect of ash percentage*

426 Comparing step 2 and step 3 UCS results, after 7 days curing, it is possible to evaluate the

427 effect of the fly ash content – 0%, 5% and 10% of the total solids weight (Figure 12). Overall,

428 the results are in agreement with those from the triaxial tests presented before, where it was

429 clear that the reduction in ash content (from 15% to 10%) represents a decrease in strength.

430 This decrease is significantly more pronounced when the ash is activated, at least after 7 days

431 curing.

432   On the other hand, it is interesting to note that the use of lime and 10% fly ash

433 represents a strength decrease relatively to the use of lime alone. This is contrary to the results

434 of Consoli et al. (2011b), that reported a significant strength increase when 12,5% and 25%

435 ash were added to distinct lime percentages (from 3% to 9%), when stabilizing a similar soil,

436 using very similar fly ash, in terms of chemical composition. This suggests the possibility of

437 existing a minimum ash content in order to take full advantage of the pozzolanic effect of the

438 ash. On the other hand, pozzolanic effects on strength require an extended curing period to be

439 fully noticeable. It is possible that, for higher curing periods (when there is enough time to

440 take full advantage of the added fly ash), the strength of the soil + lime + ash + water

441 mixtures will increase linearly with the ash content. This is not noticeable at this early curing

442 period of 7 days, where the overall particle size distribution might be prevalent in terms of

443 UCS. Assuming that this second hypothesis is indeed correct, the gap between activated and

444 non-activated mixtures will probably be reduced with time. Although both mixtures have ash

445 and calcium required to develop pozzolanic reactions, in the case of the activated mixtures

446 there is also a N-A-S-H gel type forming, which will hinder the development of calcium-

447 based reactions after medium to long term curing periods.

448

449   *Comparison of different binders*

450   Figure 13 compares the different binders considered: lime; activated ash; lime and ash; lime

451   and activated ash; and OPC with RoadCem. As it was already observed in previous figures,

452   the activated ash mixed with lime always showed the best performance, both in terms of final

453   (28 days) strength and in terms of strength gain rate. Somehow surprisingly, the OPC +

454   RoadCem mixture showed a rather slow strength increase, when compared with the remaining

455   mixtures. However, it should be taken in consideration that the relative dosage might have a

456   strong impact on these results, i.e., to have comparable strength values a higher dosage of

457   OPC and RoadCem® might be necessary. On the other hand, the OPC content was already

458   significant (8% and 12%), indicating that for the same strength values the use of alkali-

459   activated ash may be more economic.

460

461   **Conclusions**

462   The paper compares the performance of different binders, based mainly on lime and fly ash,

463   with or without alkaline activation as the liquid phase. It is highlighted that the alkaline

464   activation reaction kinetics may be improved or reduced depending on the mixture

465   composition. Lime, ash, sodium chloride and the alkaline activator were used in different

466   combinations and compared to Portland cement and a specific new additive, recently available

467   in the market for road applications. The following conclusions may be taken:

468   • The lime + activated ash mixtures were the most performing in terms of uniaxial

469   compression strength and axial stiffness;

470   • The sodium chloride significantly improved the lime and lime-ash mixtures, but

471   provided only a slight improvement in the activated ash mixtures;

472   • A 5% increase (from 10% to 15% in terms of solids weight) in lime content

473   represented an important strength increase after 28 days, for the lime-based mixtures,

474   for the lime and no activated ash mixtures and for the lime and activated ash mixtures.

475   Stress-strain curves and strength envelopes obtained in triaxial tests for the best

476   performing mixtures (with lime and activated ash) showed a typical strong cemented

477   soil behaviour with friction angles above 50º and cohesion intercepts higher than

478   500kPa.

479   • Considering the existing design guidelines for roads, the soil-lime mixtures studied in

480   this work did not fulfil the necessary requirements, while the soil-lime-ash mixtures

481   stay above the minimum values even without the activator. For higher performances,

482   corresponding to higher-class treated layers as expressed in GTS (2000), activated ash

483   mixtures are needed.

484

485 From the results obtained it is possible to conclude that alkali activated binders, based on low-

486 calcium fly ash, can be very competitive with cement, regarding soil stabilisation for transport

487 infrastructures applications. If the calcium content of the original fly ash is increased using an

488 additional component like lime, not only the strength gain rate is enhanced, but the final

489 strength is also improved.

499 **References**

500 Al-Mukhtar, M., A. Lasledj & J. F. Alcover (2014). Lime consumption of different clayey
501   soils. Applied Clay Science, 95,133-145. doi:10.1016/j.clay.2014.03.024

502 Arulrajah, A., Mohammadinia, A., Phummiphan, I., Horpibulsuk, S., & Samingthong, W.
503   (2016). Stabilization of Recycled Demolition Aggregates by Geopolymers comprising
504   Calcium Carbide Residue, Fly Ash and Slag precursors. Construction and Building
505   Materials, 114, 864-873.
506 ASTM (2011). D 2487- 11: Standard Practice for Classification of Soils for Engineering
507   Purposes (Unified Soil Classification System). Vol. 04.08. United States
508 ASTM (2015). C 618-15: Standard Specification for Coal Fly Ash and Raw or Calcined
509   Natural Pozzolan for Use in Concrete. Vol. 04.02. United States
510 Bahar, R., M. Benazzoug & S. Kenai (2004). Performance of compacted cement-stabilised
511   soil. Cement and Concrete Composites, 26(7), 811-820.
512   doi:10.1016/j.cemconcomp.2004.01.003
513 Basha, E. A., Hashim, R., Mahmud H. B., Muntohar A. S. (2005). Stabilization of residual
514   soil with rice husk ash and cement. Construction and Building Materials, 19(6), 448-
515   453. doi:10.1016/j.conbuildmat.2004.08.001
516 Bui, P. T., Ogawa, Y., Nakarai K, Kawai K. (2015). Effect of internal alkali activation on
517   pozzolanic reaction of low-calcium fly ash cement paste. Materials and Structures, 1-
518   15. DOI 10.1617/s11527-015-0703-6
519 Camacho-Tauta, J. F., G. Cascante, A. Viana da Fonseca, and J. A. Santos. (2015). "Time and
520   frequency domain evaluation of bender element systems." Géotechnique 65, no. 7
521   548-562.CEN (2003a). EN 13286-41 - Unbound and hydraulic bound mixtures. Test
522   method for the determination of the compressive strength of hydraulically bound
523   mixtures, Comité Européen de Normalisation, Bruxelles
524 CEN (2003b). EN 12504-4 Testing concrete – Part 4: Determination of ultrasonic pulse
525   velocity. Comité Européen de Normalisation, Bruxelles
526 CEN (2004a). EN 13286-53 – Unbound and hydraulically bound mixtures – Part 53: Methods
527   for the manufacture of test specimens of hydraulically bound mixtures using axial
528   compression, Comité Européen de Normalisation, Bruxelles
529 CEN (2004b) ISO/TS 17892-9 – Geotechnical investigation and testing – Laboratory testing
530   of soil – Part 9: Consolidated triaxial compression tests on water saturated soil,
531   Comité Européen de Normalisation, Bruxelles
532 Consoli, N., Rosa, D.A., Cruz, R.C., Dalla-Rosa, A. (2011a). Water content, porosity and
533   cement content as parameters controlling strength of artificially cemented silty soil,
534   Engineering Geology, 122(3–4), 328–333. doi:10.1016/j.enggeo.2011.05.017

535   Consoli, N., Dalla-Rosa, A. & Saldanha, R. (2011b). Variables Governing Strength of
536   Compacted Soil-Fly Ash-Lime Mixtures. Journal of Materials in Civil Engineering,
537   23(4), 432-440. doi: 10.1061/(ASCE)MT.1943-5533.0000186, 432-440.

538   Cristelo, N., Glendinning, S. & Jalali, S. (2009). Sub-Bases Layers of Residual Granite Soil
539   Stabilised with Lime. Soils and Rocks, 32(2), 83-88

540   Cristelo, N., Glendinning, S. & Teixeira Pinto, A. (2011). Deep soft soil improvement by
541   alkaline activation. Ground Improvement 164(GI2), 73-82. doi:10.1680/grim.900032

542   Cristelo, N., Glendinning, S., Miranda, T., Oliveira, D. and Silva, R. (2012a). Soil
543   stabilisation using alkaline activation of fly ash for self-compacting rammed earth
544   construction. Construction and Building Materials, 36, 727-735.
545   doi:10.1016/j.conbuildmat.2012.06.037

546   Cristelo, N., Glendinning, S., Fernandes, L., Teixeira Pinto, A. (2012b). Effect of calcium
547   content on soil stabilisation with alkaline activation. Construction and Building
548   Materials, 29, 167-174. doi:10.1016/j.conbuildmat.2011.10.049

549   Cristelo, N., Glendinning, S., Fernandes, L., Teixeira Pinto, A. (2013). Effects of alkaline-
550   activated fly ash and Portland cement on soft soil stabilization. Acta Geotechnica, 8,
551   395-405. doi: 10.1007/s11440-012-0200-9

552   Cristelo, N., Miranda, T., Oliveira, D.V., Rosa, I., Soares, E., Coelho, P., Fernandes, L.
553   (2015). Assessing the production of jet mix columns using alkali activated waste
554   based on mechanical and financial performance and CO2 (eq) emissions. Journal of
555   Cleaner Production, 102, 447-460. doi:10.1016/j.jclepro.2015.04.102

556   Dombrowski, K., Buchwald, A. & Weil, M. (2006). The influence of calcium content on the
557   structure and thermal performance of fly ash based geopolymers. Journal of Materials
558   Science, 42(9), 3033-3043. doi: 10.1007/s10853-006-0532-7

559   Elkady, T.Y. (2016). The effect of curing conditions on the unconfined compression strength
560   of lime-treated expansive soils, Road Materials and Pavement Design, 17(1), 52-69,
561   doi: 10.1080/14680629.2015.1062409

562   Fernandez, A. and J. Santamarina (2001). Effect of cementation on the small-strain
563   parameters of sands. Canadian Geotechnical Journal, 38(1), 191-199. doi:10.1139/t00-
564   081

565   Fernández-Jiménez, A. & Palomo, A. (2005). Composition and microstructure of alkali
566   activated fly ash binder:Effect of the activator. Cement and Concrete Research,35,
567   1984–1992. doi:10.1016/j.cemconres.2005.03.003

568 Fernández-Jiménez, A., de la Torre, A.G., Palomo, A., López-Olmo, G., Alonso, M.M.,
569   Aranda, M. a. G. (2006). Quantitative determination of phases in the alkaline
570   activation of fly ash. Part II: Degree of reaction. Fuel, 85, 1960–1969
571   doi:10.1016/j.fuel.2006.04.006

572 García Lodeiro, I., D. E. Macphee, A. Palomo and A. Fernández-Jiménez (2009). Effect of
573   alkalis on fresh C–S–H gels. FTIR analysis. Cement and Concrete Research, 39(3):
574   147-153. doi: 10.1016/j.cemconres.2009.01.003

575 Garcia-Lodeiro, I., A. Palomo, A. Fernández-Jiménez and D. E. Macphee (2011).
576   Compatibility studies between N-A-S-H and C-A-S-H gels. Study in the ternary
577   diagram Na2O–CaO–Al2O3–SiO2–H2O. Cement and Concrete Research, 41(9): 923-
578   931. doi:10.1016/j.cemconres.2011.05.006

579 Garcia-Lodeiro I, Fernandez-Jimenez A and Palomo A. (2013). Variation in hybrid cements
580   over time. Alkaline activation of fly ash-Portland cement blends. Concrete Research,,
581   52,112-122. http://dx.doi.org/10.1016/j.cemconres.2013.03.022

582 Ghosh, A., & Subbarao, C. (2001). Microstructural development in fly ash modified with lime
583   and gypsum. Journal of Materials in Civil Engineering, 13(1), 65–70
584   doi:10.1061/(ASCE)0899-1561(2001)13:1(65), 65-70.

585 Goodary, R., Lecomte-Nana, G. L., Petit C., Smith D. S. (2012). Investigation of the strength
586   development in cement-stabilised soils of volcanic origin. Construction and Building
587   Materials, 28(1), 592-598. doi:10.1016/j.conbuildmat.2011.08.054

588 Goto, S., Tatuoka, F. Shibuya, S., Kim, Y.S and Sato, T. (1991). A simple gauge for local
589   small strain measurements in the laboratory. Soil and Foundations, 31(1), 169-180.
590   doi: 10.3208/sandf1972.31.169

591 GTS (2000). Guide technique pour le traitement des sols à la chaux et/ou aux liants
592   hydrauliques. Application à la réalisation des remblais et des couches de forme.
593   (Technical guide for soils treated with lime and cement, In French), LCPC/SETRA.

594 Güllü, H. (2015). Unconfined compressive strength and freeze–thaw resistance of fine-
595   grained soil stabilised with bottom ash, lime and superplasticiser, Road Materials and
596   Pavement Design, 16(3), 608-634, doi: 10.1080/14680629.2015.1021369

597 Gurbuz, A. (2015). Marble powder to stabilise clayey soils in sub-bases for road construction,
598   Road Materials and Pavement Design, 16(2), 481-492,
599   doi:10.1080/14680629.2015.1020845

600 Han, C. & Cheng, P. (2015). Micropore variation and particle fractal representation of lime-
601   stabilised subgrade soil under freeze–thaw cycles, Road Materials and Pavement
602   Design, 16(1), 19-30, doi:10.1080/14680629.2014.956139

603 Hoy, M., Horpibulsuk, S., & Arulrajah, A. (2016). Strength development of Recycled Asphalt
604   Pavement–Fly ash geopolymer as a road construction material. Construction and
605   Building Materials, 117, 209-219.

606 Horpibulsuk, S., Katkan, W., Sirilerdwattana, W., Rachan R. (2006). Strength development in
607   cement stabilized low plasticity and coarse grained soils: laboratory and field study.
608   Soils and Foundations, 46(3), 351-366. doi: 10.3208/sandf.46.351

609 Ingles, O. G. & Metcalf, J. B. 1972. Soil stabilization: principles and practice. Butterworths,
610   Sydney – Melbourne – Briesbane.

611 JAE (1995). Pavement design manual for the national road network. Junta Autónoma de
612   Estradas (in Portuguese)

613 Juenger, M. C. G., Winnefeld, F., Provis, J. L., Ideker J. H. (2011). Advances in alternative
614   cementitious binders. Cement and Concrete Research, 41(12), 1232-1243.
615   doi:10.1016/j.cemconres.2010.11.012

616 Kamei, T., Ahmed A. & Ugai K. (2013). Durability of soft clay soil stabilized with recycled
617   Bassanite and furnace cement mixtures. Soils and Foundations, 53(1), 155-165.
618   doi:10.1016/j.sandf.2012.12.011

619 Kaniraj, S. R. and Havanagi, V. G. (1999). Compressive strength of cement stabilized fly ash-
620   soil mixtures. Cement and Concrete Research, 29(5), 673-677. doi:10.1016/S0008-
621   8846(99)00018-6

622 Khemissa, M. & A. Mahamedi (2014). Cement and lime mixture stabilization of an expansive
623   overconsolidated clay. Applied Clay Science, 95, 104-110.
624   doi:10.1016/j.clay.2014.03.017

625 Kolias, S., Kasselouri-Rigopoulou V. & Karahalios A. (2005). Stabilisation of clayey soils
626   with high calcium fly ash and cement. Cement and Concrete Composites, 27(2), 301-
627   313. doi:10.1016/j.cemconcomp.2004.02.019

628 Kua, T. A., Arulrajah, A., Horpibulsuk, S., Du, Y. J., & Shen, S. L. (2016). Strength
629   assessment of spent coffee grounds-geopolymer cement utilizing slag and fly ash
630   precursors. Construction and Building Materials, 115, 565-575.

631 Kumar, A., Walia, B., & Bajaj, A. (2007). Influence of Fly Ash, Lime, and Polyester Fibers
632   on Compaction and Strength Properties of Expansive Soil. Journal of Materials in

Civil Engineering, 19(3), 242-248, doi: 10.1061/(ASCE)0899-1561(2007)19:3(242), 242-248

Little and Nair (2009). Recommended practice for stabilization of subgrade soils and base materials. National Cooperative Highway Research Program, Transportation Research Board of National Academies, USA

Little, D. (1995). Handbook for stabilisation of pavement subgrades and base courses with lime. Lime association of Texas, USA

Little, D., Nair, S., & Herbert, B. (2010). Addressing Sulfate-Induced Heave in Lime Treated Soils. Journal of Geotechnical and Geoenvironmental Engineering, doi:10.1061/(ASCE)GT.1943-5606.0000185, 110-118.

Marjanovic, P., Egyed, C.E.G., de La Roij, P. and de La Roij, R. (2009). The Road to the Future. Manual Working with RoadCem. PowerCem Technologies B.V. The Netherlands

Mitchell, J. (1981). Soil-improvement - State-of-the-art report. Proc. 10th ICSMFE, Stockholm.

Mohammadinia, A., Arulrajah, A., Sanjayan, J., Disfani, M., Bo, M., and Darmawan, S. (2014). "Laboratory Evaluation of the Use of Cement-Treated Construction and Demolition Materials in Pavement Base and Subbase Applications." J. Mater. Civ. Eng., 10.1061/(ASCE)MT.1943-5533.0001148, 04014186.

Narendra, B. S., Sivapullaiah P. V. & Ramesh H. N. (2003). Optimum lime content of fly ash with salt. Proc. of the Inst. of Civil Engineers - Ground Improvement, 7(4), 187-191. doi: 10.1680/grim.2003.7.4.187

Oza, J. B. & Gundaliya, P. J. (2013). Study of Black Cotton Soil Characteristics with Cement Waste Dust and Lime. Procedia Engineering 51: 110-118. doi:10.1016/j.proeng.2013.01.017

Petry, T. & Little, D. (2002). Review of Stabilization of Clays and Expansive Soils in Pavements and Lightly Loaded Structures—History, Practice, and Future. J. Mater. Civ. Eng., 10.1061/(ASCE)0899-1561(2002)14:6(447), 447-460.

Phetchuay, C., Horpibulsuk, S., Suksiripattanapong, C., Chinkulkijniwat, A., Arulrajah, A., & Disfani, M. M. (2014). Calcium carbide residue: Alkaline activator for clay–fly ash geopolymer. Construction and Building Materials, 69, 285-294.

Phummiphan, I., Horpibulsuk, S., Sukmak, P., Chinkulkijniwat, A., Arulrajah A., Shen S.-L. (2016). Stabilisation of marginal lateritic soil using high calcium fly ash-based

geopolymer. Road Materials and Pavement Design.
doi:10.1080/14680629.2015.1132632

Provis, J., van Deventer, J. (Eds.) (2014). Alkali Activated Materials: State-of-the-art Report, RILEM TC 224-AAM. Springer

Puligilla, S. & Mondal, P. (2013). Role of slag in microstructural development and hardening of fly ash-slag geopolymer. Cement and Concrete Research, 43, 70-80. doi:10.1016/j.cemconres.2012.10.004

Ramesh H. N., Sivapullaiah, P. V. & Sivamohan, M. (1999). lmprovement of strength of fly ash with lime and sodium salts. Proc. of the Inst. of Civil Engineers - Ground Improvement, 3, 163-167.

Rao, S. & P. Acharya (2014). Synthesis and Characterization of Fly Ash Geopolymer Sand. Journal of Materials in Civil Engineering, 26(5), 912-917. doi:10.1061/(ASCE)MT.1943-5533.0000880

Rios, S., Viana da Fonseca, A. & Baudet, B. (2012). The effect of the porosity/cement ratio on the compression behaviour of cemented soil. Journal of Geotechnical and Environmental Engineering, 138(11), 1422–1426, doi: 10.1061/(ASCE)GT.1943-5606.0000698

Rios, S., Viana da Fonseca, A. and Baudet, B. (2014). On the shearing behaviour of an artificially cemented soil. Acta Geotechnica, 9(2), 215-226, doi : 10.1007/s11440-013-0242-7

Rios, S., Cristelo, C., Viana da Fonseca, A., Ferreira, C. (2015). Structural Performance of Alkali Activated Soil-Ash versus Soil-Cement. Journal of Materials in Civil Engineering, doi: 10.1061/(ASCE)MT.1943-5533.0001398.

Samaras, P., Papadimitriou, C. A., Haritou, I., Zouboulis, A. I. (2008). Investigation of sewage sludge stabilization potential by the addition of fly ash and lime. Journal of Hazardous Materials 154(1-3), 1052-1059

Saride, S., Puppala, A. J. & Chikyala, S. R. (2013). Swell-shrink and strength behaviors of lime and cement stabilized expansive organic clays. Applied Clay Science, 85, 39-45. doi:10.1016/j.clay.2013.09.008

Saride, S., Avirneni, D., & Challapalli, S. (2016). Micro-mechanical interaction of activated fly ash mortar and reclaimed asphalt pavement materials. Construction and Building Materials, 123, 424-435.

698   Scrivener, K.L., Kirkpatrick, R.J. (2008). Innovation in use and research on cementitious
699   material. Cement and Concrete Research, 38, 128-136
700   doi:10.1016/j.cemconres.2007.09.025
701   Sherwood, P. (1993). Soil stabilization with cement and lime. State of the Art Review.
702   London: Transport Research Laboratory, HMSO
703   Silva, R.A., Oliveira, D.V., Miranda, T., Cristelo, N., Escobar, M.C., Soares, E. (2013).
704   Rammed earth construction with granitic residual soils: The case study of northern
705   Portugal. Construction and Building Materials, 47(0), 181-191.
706   doi:10.1016/j.conbuildmat.2013.05.047
707   Sukmak, P., Horpibulsuk S., & Shen S.-L (2013). Strength development in clay–fly ash
708   geopolymer. Construction and Building Materials, 40(0), 566-574.
709   doi: 10.1016/j.conbuildmat.2012.11.015
710   Sukmak, P., P. D. Silva, S. Horpibulsuk and P. Chindaprasirt (2015). Sulfate Resistance of
711   Clay-Portland Cement and Clay High-Calcium Fly Ash Geopolymer. Journal of
712   Materials in Civil Engineering 27(5): 04014158.
713   Van Impe, W.F. (1989). Soil improvement techniques and their evolution, Rotterdam,
714   Balkema, Netherlands
715   Xing, H. F., Yang, X. M, Xu, C. and Ye, G. B. (2009). Strength characteristics and
716   mechanisms of salt-rich soil-cement, Engineering Geology, 103 33–38, doi:
717   http://dx.doi.org/10.1016/j.enggeo.
718   Yi, Y., C. Li and S. Liu (2015). "Alkali-Activated Ground-Granulated Blast Furnace Slag for
719   Stabilization of Marine Soft Clay." Journal of Materials in Civil Engineering 27(4):
720   04014146.
721   Yilmaz, Y. & V. Ozaydin (2013). Compaction and shear strength characteristics of
722   colemanite ore waste modified active belite cement stabilized high plasticity soils.
723   Engineering Geology, 155, 45-53. doi:10.1016/j.enggeo.2013.01.003
724   Yong, R. N. & Ouhadi, V. R. (2007). Experimental study on instability of bases on natural
725   and lime/cement-stabilized clayey soils. Applied Clay Science, 35(3–4), 238-249.
726   doi:10.1016/j.clay.2006.08.009
727   Yusuf, F., Little, D. N., & Sarkar, S. L. (2001). Evaluation of structural contribution of lime
728   stabilization of subgrade soils in Mississippi. Transportation Research Record 1757,
729   Transportation Research Board, National Research Council, Washington DC, 22–31
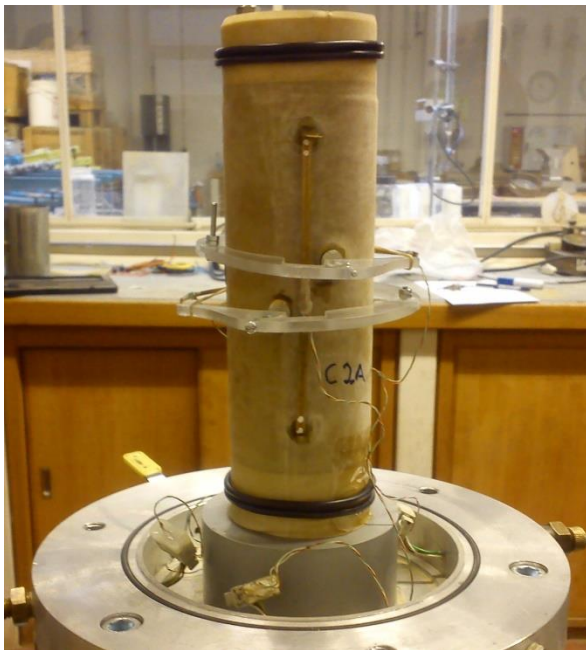
730   Zhang, M., Guo, H., El-Korchi, T., Zhang, G. & Tao, M. (2013). Experimental feasibility

731   study of geopolymer as the next-generation soil stabilizer. Construction and Building

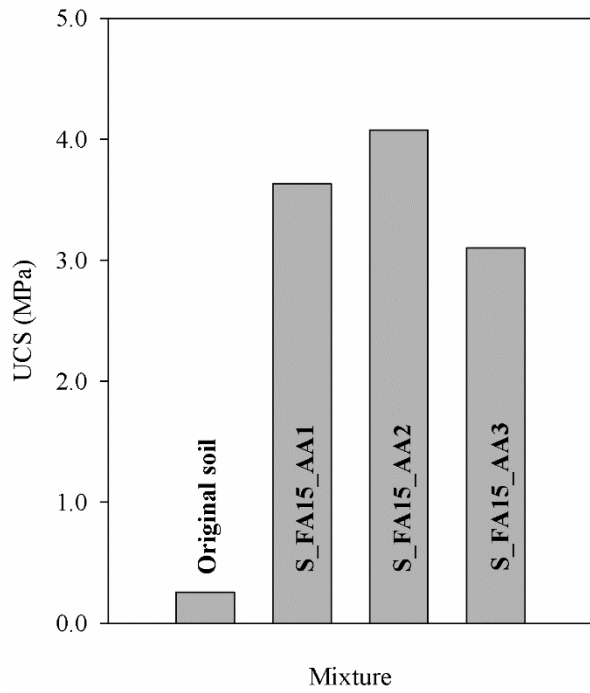732   Materials, 47(0), 1468-1478. doi: 10.1016/j.conbuildmat.2013.06.017

733
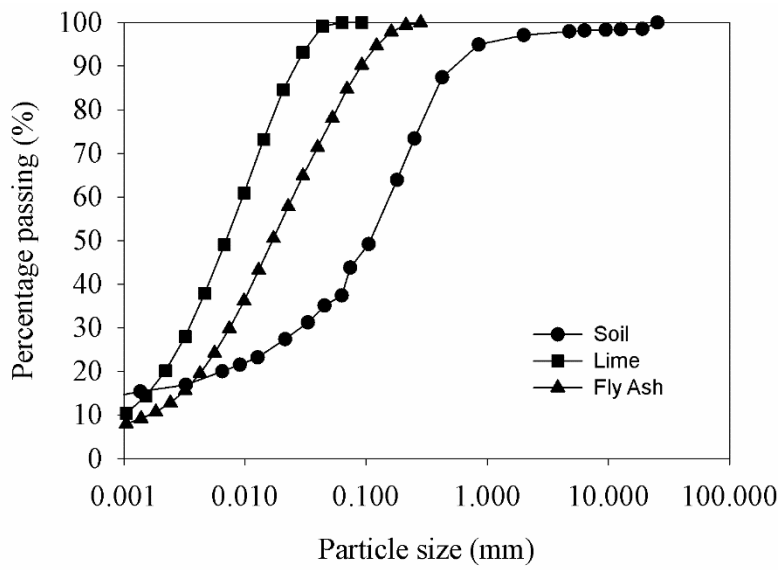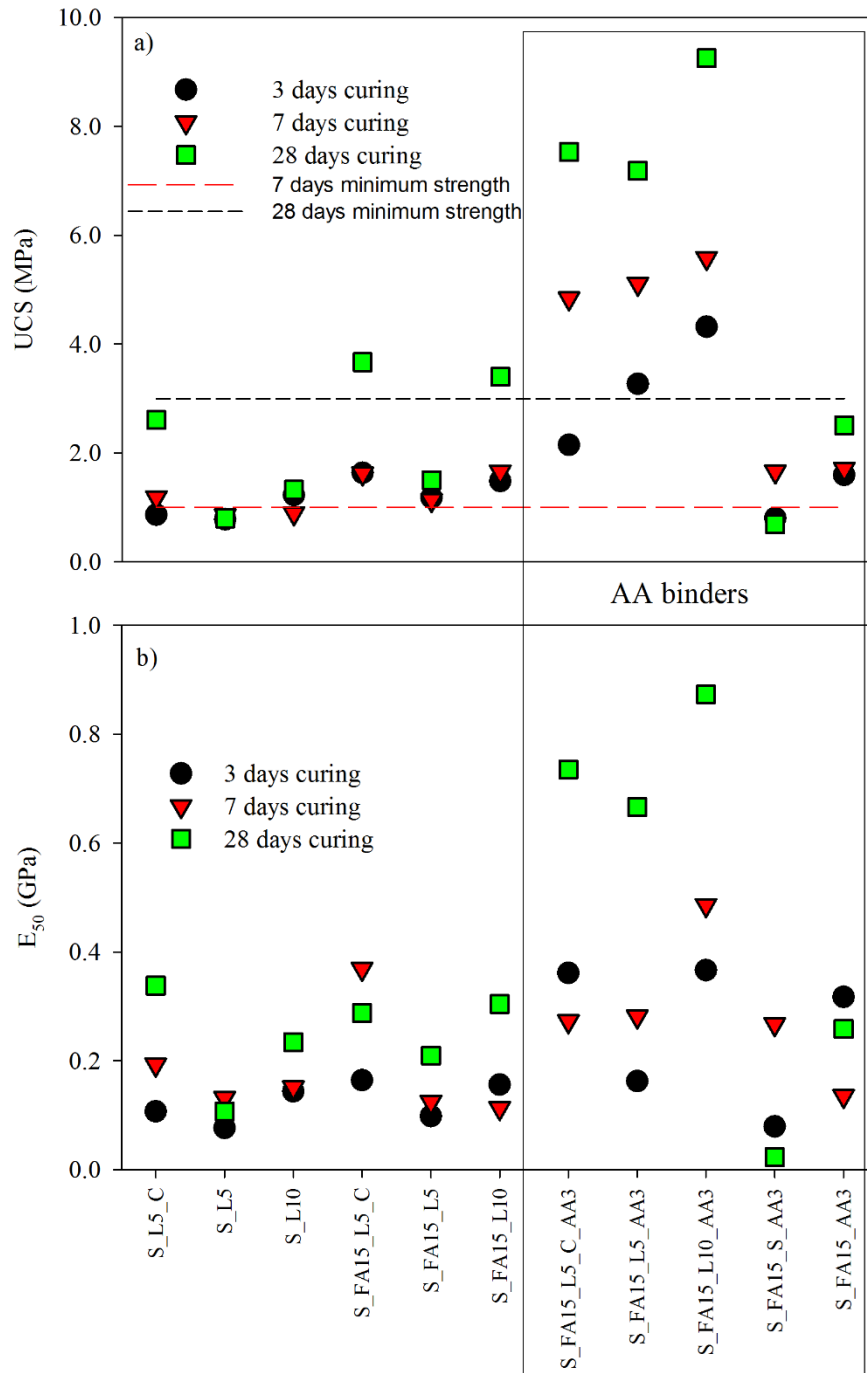
736   Figure 1 - Particle size distribution of the soil, lime and fly ash

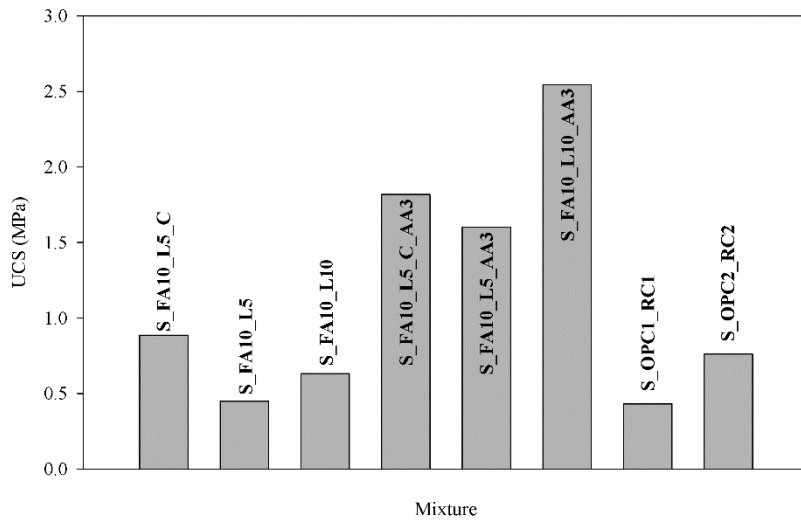738   Figure 2 - Triaxial test setup showing the Linear Displacement Transformers (LDT) sensors

739

740   Figure 3 - Step 1 UCS results (28 days curing)

Figure 4 - UCS results for step 2 (3, 7 and 28 days curing): a) unconfined compressive strength (UCS); b) Stiffness modulus at 50% of maximum strength (E_{50}) - S (soil); FA (fly ash); L (lime); C (sodium chloride); AA (alkali activated)
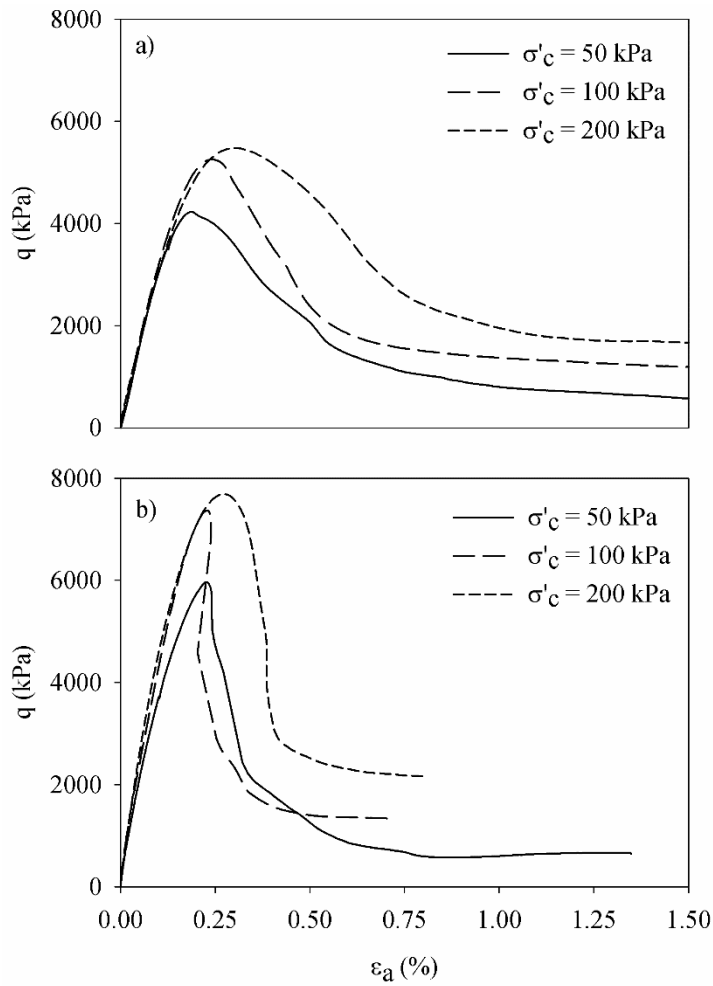
745

746   Figure 5 - UCS results for step 3 (7 days curing) - S (soil); FA (fly ash); L (lime); C (sodium

747   chloride); AA (alkali activated); OPC (Portland cement); RC (RoadCem)
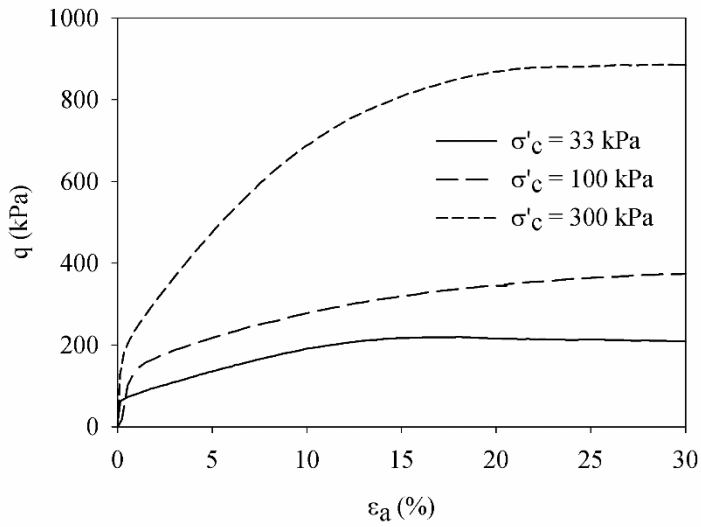
748

749   Figure 6 - Stress-strain curves obtained from the triaxial compression tests performed on the

750   original soil (σ'c refers to the isotropic consolidation stress applied)
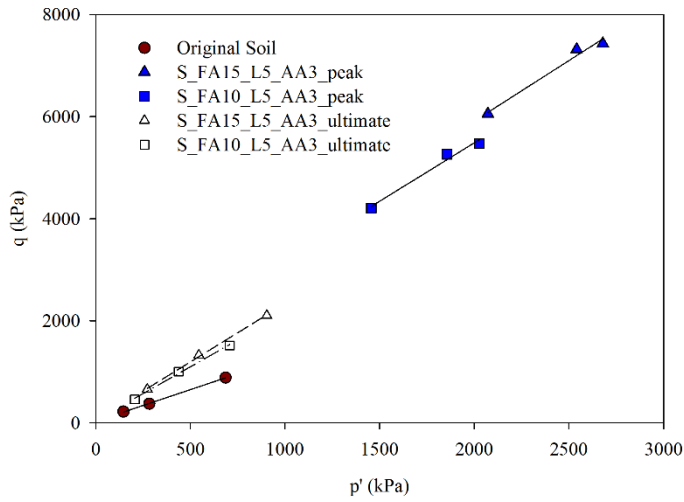
32

751

752 Figure 7 - Stress-strain curves obtained from the triaxial compression tests performed on the

753 mixtures S_FA10_L5_AA3 (a) and S_FA15_L5_AA3 (b) (σ'c refers to the isotropic

754 consolidation stress applied)
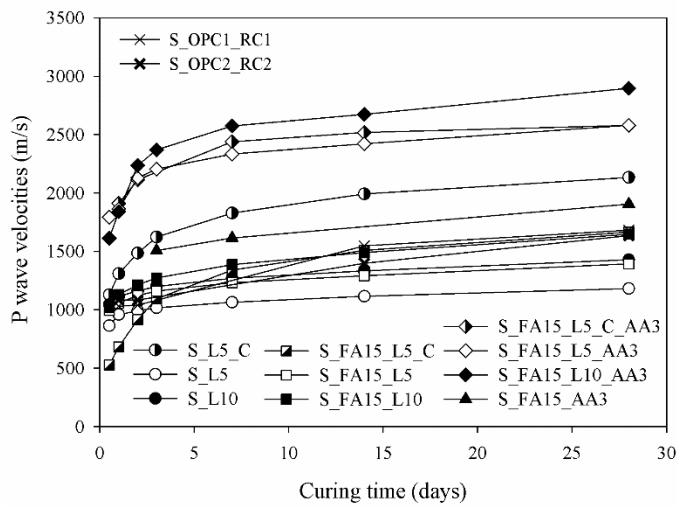
755

756 Figure 8 – P wave velocities evolution with curing time

757

758   Figure 9 - Peak and ultimate state strength envelopes (the soil specimens presented very

759   similar peak and ultimate envelops, which are not possible to distinguish at this scale)
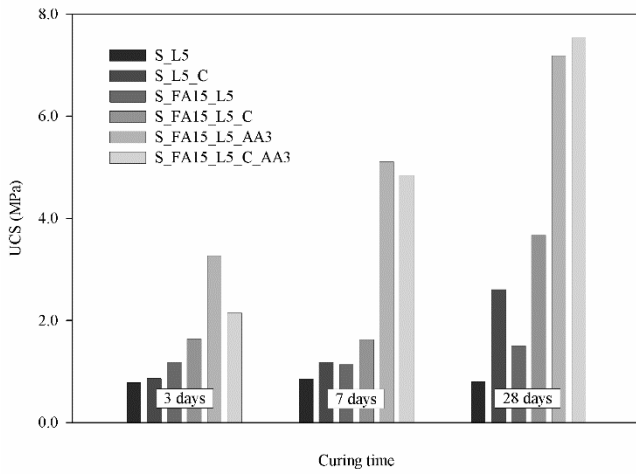
760

761   Figure 10 - Effect of sodium chloride on the uniaxial compression strength
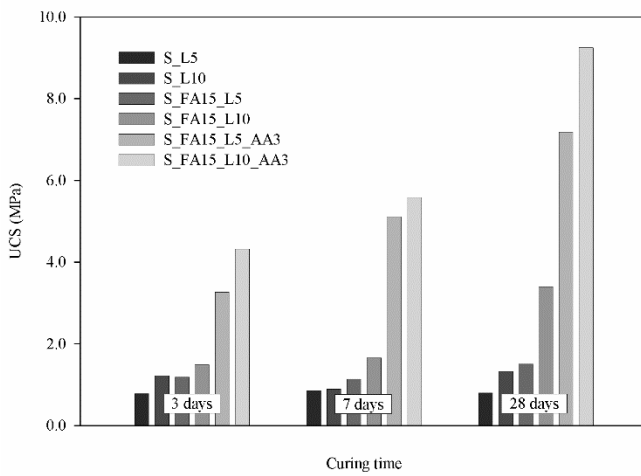
762

763   Figure 11 - Effect of lime percentage on the uniaxial compression strength

34

Figure 12 - Effect of ash percentage on the uniaxial compression strength after curing for 7 days

Figure 13 – Effect of the binder type on the uniaxial compression strength

773

774 Table 1 - Main geotechnical properties of the soil

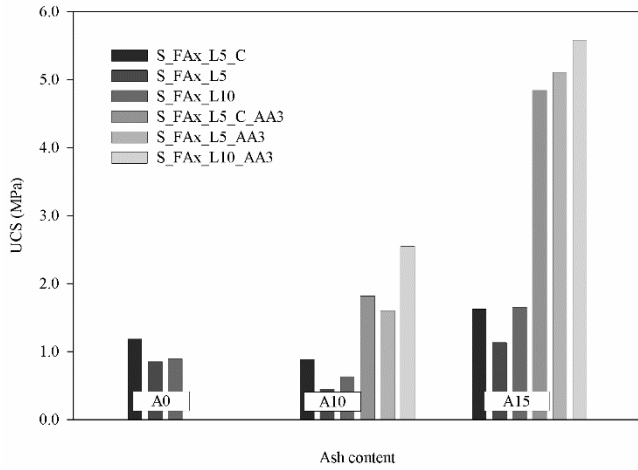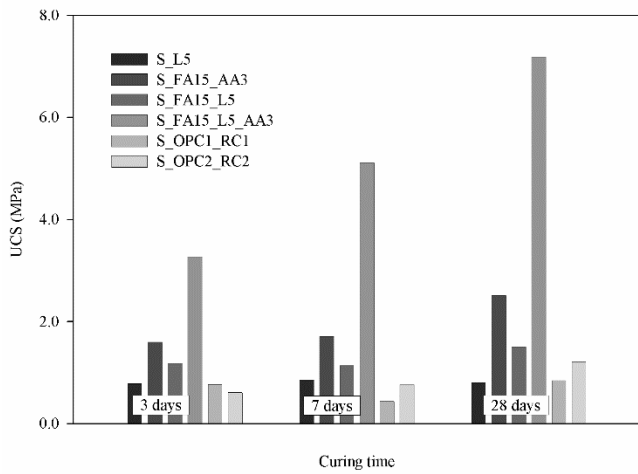| Properties	Symbol	Value
Plastic limit (%)	w_P	13.0
Liquid limit (%)	w_L	19.5
Average diameter (mm)	D_{50}	0.105
Fines fraction (sieve Nº 200) (%)	$P_{\#200}$	43.8
Uniformity coefficient	C_u	167
Curvature coefficient	C_c	6.7
Specific gravity	G	2.60
Modified Proctor test optimum water content (%)	w_{op}	8.2
Modified Proctor test maximum density (kN/m3)	γ_d	21.29
California Bearing Ratio (%)	CBR	9
Unified Soil Classification System ASTM D 2487 (2011)	-	SC-SM silty sand

775

776 Table 2: Chemical composition of the fly ash (wt%)

Element	Si	Al	Fe	Ca	K	Ti	Mg	Na	S	P
Fly ash	48.81	21.77	14.74	3.85	4.42	1.79	1.56	1.31	1.17	0.58

777 Table 3 - Identification of prepared mixtures

Step	ID	Solid Phase				Liquid Phase	
		Soil (%)	Ash (%)	Lime (%)	SC(*) (%)	Activator/ Fly ash (wt)	Water content (%)
0	Soil	100	-	-	-	-	5.0
1	S_FA15_AA1	85	15	-	-	0.943	10.4
	S_FA15_AA2	85	15	-	-	0.825	9.1
	S_FA15_AA3	85	15	-	-	0.707	7.8
2	S_L5_C	94	-	5	1	-	5.0
	S_L5	95	-	5	-	-	5.0
	S_L10	90	-	10	-	-	5.0
	S_FA15_L5_C	79	15	5	1	-	5.0
	S_FA15_L5	80	15	5	-	-	5.0
	S_FA15_L10	75	15	10	-	-	5.0
	S_FA15_C_AA3	84	15	-	1	0.707	7.8
	S_FA15_AA3	85	15	-	-	0.707	7.8
	S_FA15_L5_C_AA3	79	15	5	1	0.707	7.8
	S_FA15_L5_AA3	80	15	5	-	0.707	7.8
	S_FA15_L10_AA3	75	15	10	-	0.707	7.8
3	S_FA10_L5_C	84	10	5	1	-	5.0
	S_FA10_L5	85	10	5	-	-	5.0
	S_FA10_L10	80	10	10	-	-	5.0
	S_FA10_L5_C_AA3	84	10	5	1	1.06	7.8
	S_FA10_L5_AA3	85	10	5	-	1.06	7.8
	S_FA10_L10_AA3	80	10	10	-	1.06	7.8
	S_OPC1_RC1	92	8% OPC + 0.08% RC			-	5.0
	S_OPC2_RC2	88	12% OPC + 0.11% RC			-	5.0

778 (*) SC stands for sodium chloride

779

780

781

782   Table 4 – Tests performed in each mixture and corresponding curing time

Step	ID	Curing time of the specimens tested in:		
		UCS	Triaxial tests	Seismic waves
0	Soil	0	0	
1	S_FA15_AA1	28		
	S_FA15_AA2	28		
	S_FA15_AA3	28		
2	S_L5_C	3, 7, 28		12, 24 and 48 h + 3, 7, 14 and 28 days
	S_L5	3, 7, 28		12, 24 and 48 h + 3, 7, 14 and 28 days
	S_L10	3, 7, 28		12, 24 and 48 h + 3, 7, 14 and 28 days
	S_FA15_L5_C	3, 7, 28		12, 24 and 48 h + 3, 7, 14 and 28 days
	S_FA15_L5	3, 7, 28		12, 24 and 48 h + 3, 7, 14 and 28 days
	S_FA15_L10	3, 7, 28		12, 24 and 48 h + 3, 7, 14 and 28 days
	S_FA15_C_AA3	3, 7, 28		
	S_FA15_AA3	3, 7		12, 24 and 48 h + 3, 7, 14 and 28 days
	S_FA15_L5_C_AA3	3, 7, 28		12, 24 and 48 h + 3, 7, 14 and 28 days
	S_FA15_L5_AA3	3, 7, 28	28	12, 24 and 48 h + 3, 7, 14 and 28 days
	S_FA15_L10_AA3	3, 7, 28		12, 24 and 48 h + 3, 7, 14 and 28 days
3	S_FA10_L5_C	7		
	S_FA10_L5	7		
	S_FA10_L10	7		
	S_FA10_L5_C_AA3	7		
	S_FA10_L5_AA3	7	28	
	S_FA10_L10_AA3	7		
	S_OPC1_RC1	3, 7, 28		12, 24 and 48 h + 3, 7, 14 and 28 days
	S_OPC2_RC2	3, 7, 28		12, 24 and 48 h + 3, 7, 14 and 28 days

783

784   Table 5 - Stiffness modulus at 50% of the deviatoric stress (E_{50}). Results in MPa

Mixture	Confining pressure of 33 (soil) or 50 kPa (mixtures)	Confining pressure of 100 kPa	Confining pressure of 300 (soil) or 200 kPa (mixtures)
Soil	3.68	6.84	10.21
S_FA10_L5_AA3	3194.3	3299.7	3154.3
S_FA15_L5_AA3	3901.1	4392.1	4759.9

785

786   Table 6 – Mohr Coulomb failure criteria parameters

Mixture	Peak		Ultimate strength	
	ϕ' (°)	c' (kPa)	ϕ' (°)	c' (kPa)
Soil	31	15	32	0
S_FA10_L5_AA3	56	587	49	27
S_FA15_L5_AA3	58	796	56	33

787